

A review of instability criteria of smoke layers under sprinkler spray

K.Y. Li^{*}, M.J. Spearpoint

Department of Civil and Natural Resources Engineering,
University of Canterbury,
Christchurch 8140, New Zealand

ABSTRACT

Three different criteria have been developed to determine the smoke layer behavior under sprinkler spray and these are known as the Bullen criterion, the Zhang criterion and the Li criterion. A review is carried out theoretically and experimentally to validate these criteria. The experimental results have shown that the values of all three criteria are less than unity when a smoke layer is stable under sprinkler spray, but only the Li criterion becomes greater than unity after smoke logging occurs. When the three criteria are physically compared the results show that the spatial distribution has a significant impact on the smoke layer behavior and also determines the shape of the smoke logging plume.

Keywords

Sprinkler spray; smoke logging; drag force; buoyancy; smoke layer.

1. INTRODUCTION

Previous researchers [1-5] have found that a smoke layer is affected by sprinkler spray mainly by drag and cooling effect. As a result, the layer instability leads to smoke contamination to the lower fresh air [4, 5] and reduces the efficiency of any smoke venting system [6]. The smoke layer instability is referred to as “smoke logging” by Cooper [4, 5] and this term is also applied to describe the smoke behavior in this study.

Compared to the cooling effect, the drag effect has a more significant impact on smoke logging as the smoke that activates the sprinkler would have a relatively high temperature. Usually the cooling effect can only reduce the temperature to a certain range under which the smoke layer remains stable due to its buoyancy. However, the drag force produced by the droplets pulls the smoke down in spite of the buoyancy. As long as the drag force exceeds the buoyancy, the smoke layer loses its stability and the smoke moves downwards towards the floor. Three criteria have been developed to reveal the mechanisms of smoke logging and these are referred to as the Bullen criterion [1], the Zhang criterion [2] and the Li criterion [3]. In this study, a review of these criteria is conducted. The physical mechanism of each criterion is also analyzed. Several experimental results are applied in order to determine which criterion is more appropriate compared to the others.

* Corresponding author - tel (64) 3 3642987 extension 7327; fax (64) 3 3642758; email address kai.yuan-li@canterbury.ac.nz

2. LITERATURE REVIEW

2.1 Bullen criterion

Bullen investigated smoke logging under sprinkler spray with a criterion developed in 1974. The criterion was used to determine whether smoke logging would occur under certain sprinkler spray conditions. In his theory, a smoke layer is assumed to have a constant depth. The sprinkler spray was taken to be characterized by water droplets with a constant diameter and this diameter was calculated from the sprinkler pressure. A physical parameter known as the ‘drag-to-buoyancy ratio’ was calculated for the entire smoke layer to assess its stability. As shown in Figure 1, the smoke layer is assumed to be stable under sprinkler spray. The total drag force of sprinkler spray acting on the smoke layer is considered. The drag force generated by each droplet is summed to calculate the total drag force, which can be expressed as

$$D_t = \dot{M} \left(\frac{m_d g}{k_d} \right)^{1/2} \left\{ \frac{1}{2} \ln \left[\frac{1 + \left[1 - \exp\left(-\frac{2k_d h}{m_d}\right) \right]^{1/2}}{1 - \left[1 - \exp\left(-\frac{2k_d h}{m_d}\right) \right]^{1/2}} \right] - \left[1 - \exp\left(-\frac{2k_d h}{m_d}\right) \right]^{1/2} \right\} \quad (1)$$

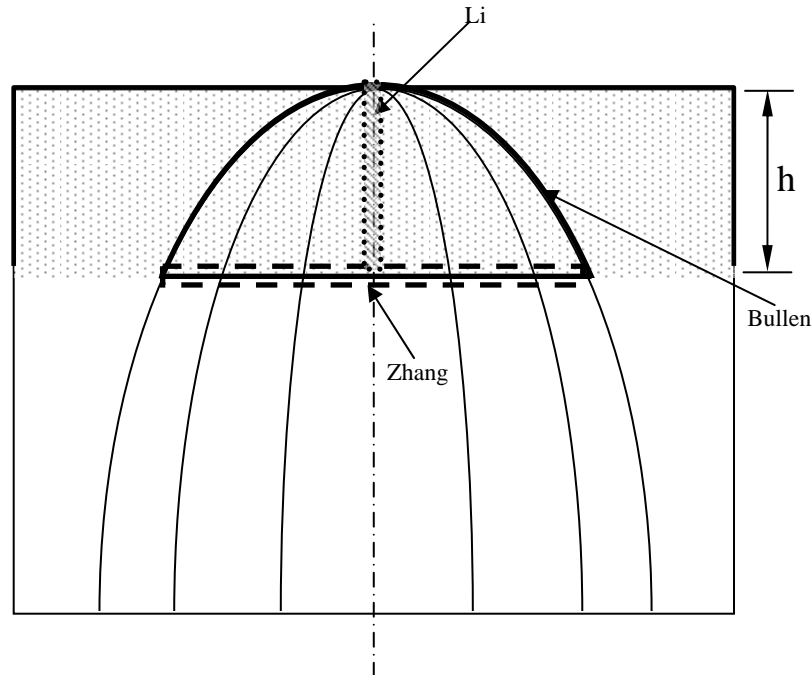


Figure 1. Schematic view of the three different stability criteria.

The buoyancy of the smoke layer in the spray region is calculated using the temperature rise and the volume of the smoke layer interacting with the sprinkler spray. The total buoyancy is calculated to be

$$B_t = \frac{3}{2} \pi \frac{\overline{\Delta T}}{\Delta T + T_0} \rho_0 g h^2 \quad (2)$$

The values of D_t and B_t are compared by using the ratio D_t/B_t . According to Bullen, the smoke layer loses its stability when $D_t/B_t > 1$, i.e. the total drag force is greater than the total buoyancy. The criterion was experimentally studied by Chow and Tong [7]. The experimental results showed that critical value of D_t/B_t to determine the occurrence of smoke logging is around 0.6, which means Bullen's criterion has under-predicted the drag effect and therefore needs to be re-evaluated.

2.2 Zhang criterion

Zhang points out that the temperature gradient of the smoke layer, which had been ignored by Bullen, significantly affects the interaction of a smoke layer and sprinkler spray. As reported by Zhang, experimental data have shown that the temperature profile of the smoke layer under sprinkler spray is approximately linear. As a result, the smoke at the smoke-air interface, which is highlighted in Figure 1 with a dash rectangle, has the lowest temperature rise compared to the upper part of the smoke layer. Based on this, the smoke element of unit volume at this location was considered, with its buoyancy calculated. The drag force of sprinkler spray on the interface was calculated to compare to the buoyancy. The drag force and the buoyancy are labeled by D_L and B_L respectively, which can be expressed as

$$D_L = \frac{\dot{M}}{\pi E x} \sqrt{\frac{3\rho_g(x)C_D g}{4\rho_d d_m} \left[1 - \exp\left(-\frac{6\rho_g(x)C_D x}{4\rho_d d_m}\right) \right]} \quad (3)$$

$$B_L = \frac{T_L - T_0}{T_L} \rho_0 g \quad (4)$$

Therefore the smoke logging state is determined from D_L/B_L . In Zhang's research, the smoke behavior that resulted from the interaction of smoke layer and sprinkler spray was defined by three different phases: smoke stable, smoke logging and smoke downdrag, in terms of different values of D_L/B_L . According to his experiment results, the critical value for smoke logging was increased to 0.8 which is still less than 1. The "bowl" shape of the smoke logging plume, which was commonly observed in the experiments, was not clearly explained by Zhang.

2.3 Li criterion

Li studied the interaction of a smoke layer and sprinkler spray theoretically and experimentally. His investigation considered the spatial distribution of the drag force in the spray region. As shown in Figure 1, a smoke column element of unit area was studied. As the envelope curve of the spray region is approximately parabolic [8], the length of the smoke column element directly below the sprinkler is greater than the others. Therefore, this element has the highest drag force, which is calculated and expressed as

$$D_0 = \int_0^h \left[\frac{\dot{M}}{\pi E x} \times \frac{3\rho_g(x)C_D}{4\rho_d d_d} \sqrt{\frac{4\rho_d d_d g}{3\rho_g(x)C_D} + C_1 \exp\left(-\frac{6\rho_g(x)C_D x}{4\rho_d d_d}\right)} \right] dx \quad (5)$$

To calculate the buoyancy of the element, the average temperature of the smoke layer was taken so that the buoyancy of smoke column element directly below the sprinkler is

$$B_0 = \frac{\overline{\Delta T}}{\overline{\Delta T} + T_0} \rho_0 g h \quad (6)$$

The drag force and the buoyancy on the element can be compared to each other by the ratio of D_0 / B_0 . When this value is greater than unity it means the drag force is greater than the buoyancy and the element moves downwards to represent a smoke logging condition. In his physical model, Li also explains the shape of the smoke logging plume “bowl” as the drag force of the sprinkler spray decreases with the radial distance away from the centerline of the spray region.

3. EXPERIMENTS

A series of experiments was conducted to validate the three different stability criteria. The experimental set up is shown in Figure 2. It consisted of two parts: the burning cabin and the sprinkler cabin.

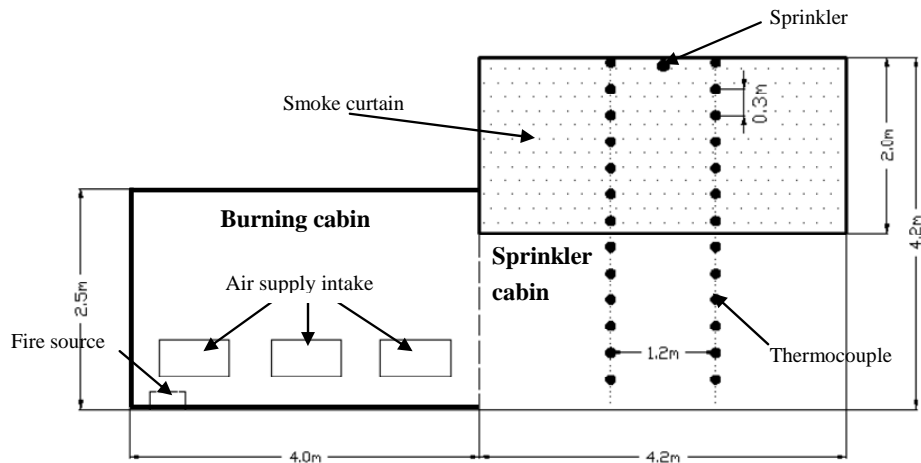


Figure 2. Schematic and photograph of the experimental rig.

Pool fires were located in the burning cabin to generate an initial stable smoke layer in the upper region. The burning cabin was 4 m long, 2 m wide and 2.5 m high. Six air supply intakes with 0.8 m x 0.4 m opening area were located on both sides of the cabin. The sprinkler cabin was a cube with an identical length, width and height of 4.2 m. A smoke curtain with depth of 2.0 m or 1.2 m was installed below the top of the cabin to maintain an initial stable smoke layer. A 4.2 m high gauge was placed in front of the cabin to measure the depth of the downward smoke plume as shown in Figure 2(b). Four thermocouple trees were distributed in a circle of 1.2 m diameter with the sprinkler at the center. The vertical interval of the thermocouples was 0.3 m. Bare bead K-type thermocouples were used with uncertainties estimated to be of less than ± 2 °C. The thermocouples were protected by steel saddle waterproofing caps to prevent the water droplets influencing the temperature measurement measured by the thermocouple bead.

A ZSTP-15 Copper Alloys spray sprinkler with nozzle diameter of 12.7 mm and a flow rate coefficient of $80 \text{ L}/(\text{min} \cdot \sqrt{\text{bar}})$ was used for the experiments. The sprinkler was installed in the center of the sprinkler cabin roof in a pendant orientation. A pressure reducing valve and pressure transmitter were installed in the pipeline to control the sprinkler operating pressure with an accuracy of 0.002 MPa. A digital video camera was used to record the experiments.

A total of 14 experiments were conducted with three different fire heat release rates. Diesel was used as the fuel for the pool fires. The heat release rate was determined by the mass loss rate measured by an electronic balance and the heat value of the diesel which was taken to be 42 MJ/kg. A burning efficiency factor of 0.8 was used which had been obtained from previous research using the cabin [9]. As a result, heat release rates used in experiment were calculated to be 200 kW, 248 kW and 476 kW for the three pool fires. In experiment, the sprinkler was activated when the upper part of the sprinkler cabin was filled with a stable smoke layer. The total burning time of each experiment was about 300 s. The operating pressure of the sprinkler varied from 0.03 to 0.07 MPa.

4. RESULTS AND DISCUSSION

4.1 Stable smoke layer

The upper part of the sprinkler cabin was filled with smoke after ignition without sprinkler spray for 50~60 s after which the smoke started to flow out of the cabin through the bottom edge of the draft curtain. The sprinkler was manually operated at 50 s. When the operating pressure was relatively low, the smoke layer would remain stable. Under this condition, the two zone structure of the smoke layer was not broken as the smoke layer temperature was relatively high.

Figure 3 presents the typical results for selected experiments without smoke logging. The interface between the smoke and the air was clearly visible in the sprinkler cabin. The depth of the smoke layer increased slightly due to the dilution effects of the water droplets in the layer. The depth increases were less than 0.3 m in all of the experiments under this condition.

The experimental data are summarized in Table 1. Using the experimental data, the three criteria are also calculated and recorded in Table 1 such that when the smoke layer remains stable all three criteria are less than unity. A photograph for experiment C1 has

not been shown in this paper however it was observed that smoke logging did not occur as would be expected when compared with experiment C2 where the operating pressure was higher.



Figure 3. Smoke layer remains stable.

Table 1. Summary of the experiments and layer stability criteria.

| Expt no. | HRR (kW) | Depth of smoke layer (m) | Sprinkler operating pressure (MPa) | Ambient temp. (K) | Average temp. rise of smoke layer (K) | Temp. rise at the smoke-air interface $T_L - T_0$ (K) | Bullen D_i / B_i | Zhang D_L / B_L | Li D_0 / B_0 | Smoke logging during expt. |
|----------|----------|--------------------------|------------------------------------|-------------------|---------------------------------------|---|--------------------|-------------------|----------------|----------------------------|
| A1 | 200 | 2.0 | 0.03 | 296 | 13.1 | 8.1 | 0.18 | 0.19 | 0.74 | No |
| A2 | 200 | 2.0 | 0.04 | 300 | 8.8 | 6.0 | 0.33 | 0.31 | 1.61 | Yes |
| A3 | 200 | 2.0 | 0.05 | 296 | 6.5 | 5.5 | 0.51 | 0.40 | 2.91 | Yes |
| B1 | 248 | 2.0 | 0.03 | 296 | 12.6 | 7.6 | 0.18 | 0.20 | 0.77 | No |
| B2 | 248 | 2.0 | 0.04 | 300 | 9.0 | 5.2 | 0.32 | 0.36 | 1.59 | Yes |
| B3 | 248 | 2.0 | 0.07 | 296 | 6.3 | 5.4 | 0.69 | 0.51 | 4.62 | Yes |
| C1 | 476 | 2.0 | 0.03 | 298 | 31.0 | 13.8 | 0.08 | 0.11 | 0.33 | No |
| C2 | 476 | 2.0 | 0.05 | 298 | 23.8 | 12.1 | 0.15 | 0.18 | 0.83 | No |
| C3 | 476 | 2.0 | 0.07 | 298 | 15.0 | 10.0 | 0.30 | 0.28 | 2.02 | Yes |
| D1 | 248 | 1.2 | 0.03 | 302 | 13.8 | 6.7 | 0.23 | 0.33 | 1.09 | Yes |
| D2 | 248 | 1.2 | 0.04 | 302 | 13.5 | 6.4 | 0.30 | 0.43 | 1.66 | Yes |
| E1 | 476 | 1.2 | 0.03 | 302 | 36.3 | 10.8 | 0.10 | 0.21 | 0.45 | No |
| E2 | 476 | 1.2 | 0.05 | 302 | 30.7 | 12.2 | 0.17 | 0.27 | 1.04 | Yes |
| E3 | 476 | 1.2 | 0.07 | 302 | 15.5 | 10.9 | 0.41 | 0.39 | 3.12 | Yes |

4.2 Smoke layer loses stability

The smoke layer would eventually lose its stability as the operating pressure increased. Under this condition the smoke layer temperature was relatively low and the stable two zone structure of the smoke-air layer was broken with a downward “smoke logging plume” created. The plume penetrated the interface and brought the smoke to the lower part of the cabin. Typical photographs from experiments with smoke logging are shown in Figure 4 and 5 where part of the smoke layer in the spray region has moved downwards and has formed the smoke logging plume.

As shown in Table 1, in all of the cases with smoke logging, D_i/B_i and D_L/B_L remain less than unity and only D_0/B_0 is greater than unity. This result suggests that D_0/B_0 is a more appropriate method of predicting the smoke logging behavior in these cases.

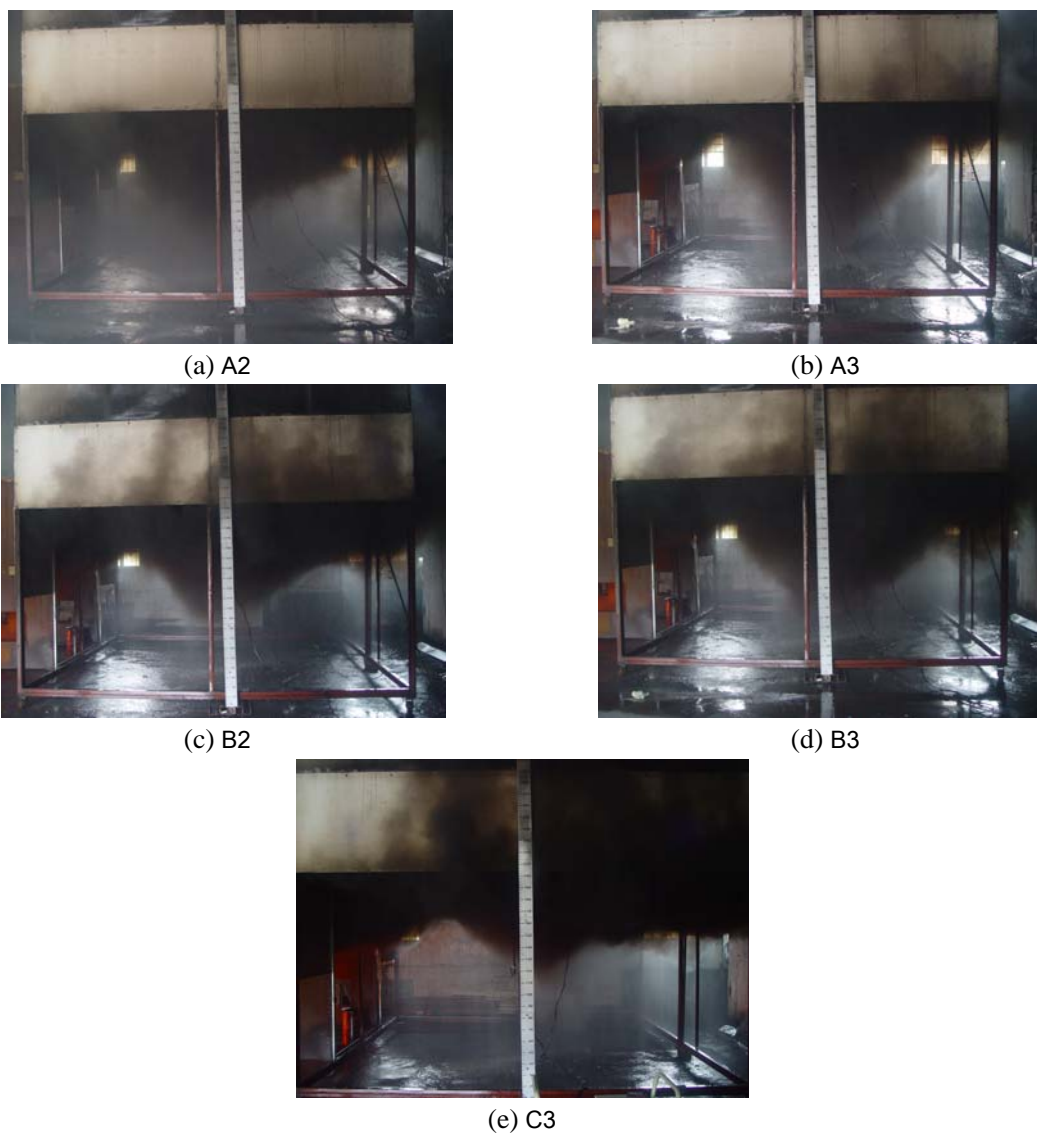


Figure 4. Smoke logging under sprinkler spray (2 m smoke curtain depth).

4.3 Discussion

The drag force and the buoyancy in the Bullen criterion is the sum of all the column elements in the spray region considered in the Li criterion. Consequently, D_t/B_t can be calculated by

$$\frac{D_t}{B_t} = \frac{\int_0^{\pi Ch} D_{x1} d\Delta}{\int_0^{\pi Ch} B_{x1} d\Delta} \quad (7)$$

where D_{x1} and B_{x1} are drag force and buoyancy of the smoke column element and $d\Delta$ is the unit area of column element. The upper limit of the integration is the area of spray region at the smoke-air interface. More details regarding D_{x1} and B_{x1} can be found in literature [3]. In fact D_{x1} is very sensitive to the height of the column, which can be calculated theoretically [3]. As it decreases from the center to the edge of spray region, and as the column height has less significant impact on the buoyancy, the value of D_{x1}/B_{x1} decreases from the center to the edge. As a result, D_t/B_t is eventually less than D_0/B_0 . Apparently, the value of D_t/B_t can be greater than unity when the operating pressure is relatively high but its critical value is definitely less than unity since the value of D_0/B_0 is around unity at the critical situation.

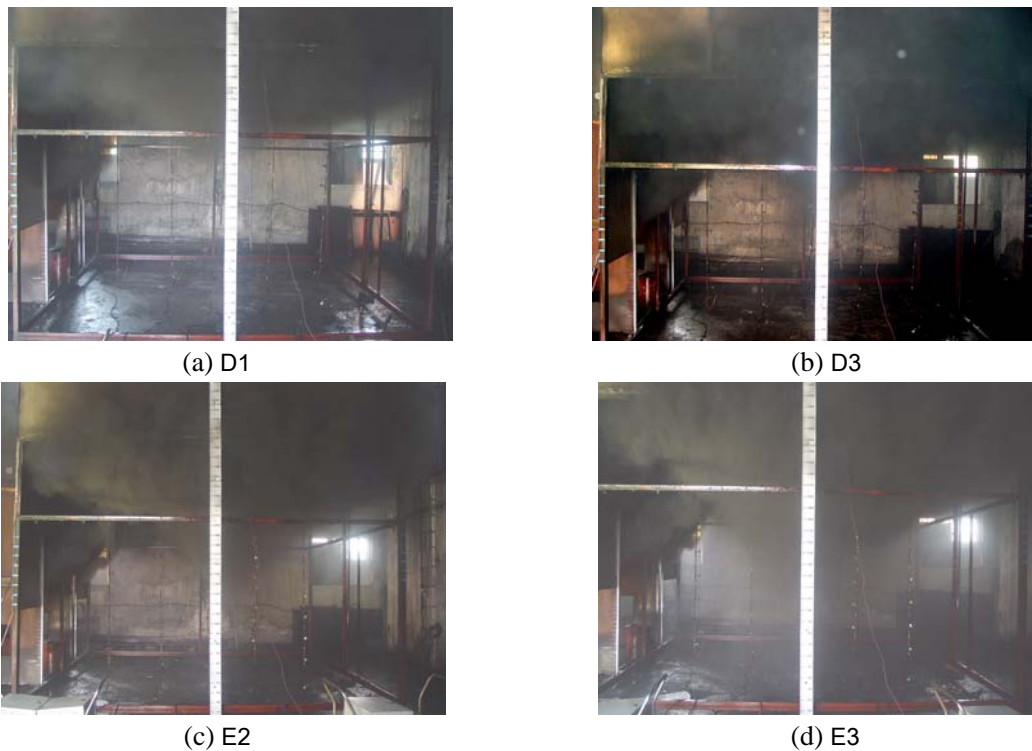


Figure 5. Smoke logging under sprinkler spray (1.2 m smoke curtain depth).

Compared to Bullen, the Zhang criterion is more accurate when the smoke layer is relatively thin but it will become less accurate as the smoke layer depth increases. This is because the drag force of unit volume decreases as the distance from sprinkler to smoke-air interface increases, thus, once the depth of smoke layer increases, the value of D_L/B_L decreases sharply. The spatial effect of the drag force has been ignored in the

Zhang criterion which has a significant influence on smoke layer stability.

According to above analysis it can be found from Table 1 that the value of D_0/B_0 is greater than the other two criteria in all experiments. The Zhang criterion gives a more accurate prediction compared to the Bullen criterion when the smoke layer is relatively thin but less accurate when the depth of smoke layer is increased.

5. CONCLUSIONS

Three different criteria for determining the smoke stability have been reviewed. The physical basis for each criterion has been analyzed with the key equations listed. A series of experiments were conducted to compare the criteria. All three of the criteria are less than unity in experiments without smoke logging. Only the Li criterion is greater than unity when smoke layer loses its stability, which means Li criterion is more appropriate for predicting the smoke logging behavior compared to the other two criteria. Furthermore, a comparison of the three criteria shows that the Li criterion has considered the spatial distribution of the drag force in the spray region. The spatial effect has a significant effect on the interaction of smoke layer and sprinkler spray which leads to the bowl shape observed in the smoke logging plume.

ACKNOWLEDGEMENT

Kai-Yuan Li is currently the Arup Fire Post-doctorate Fellow at the University of Canterbury.

REFERENCES

1. M.L. Bullen, The Effect of a Sprinkler on the Stability of a Smoke Layer Beneath a Ceiling. Fire Research Note 1016, Fire Research Station, Borehamwood, UK, pp. 1–11, 1974.
2. C.F. Zhang, Study on the Dynamics of Smoke Movement under Some Typical Sprinklers, University of Science and Technology of China, Hefei, Anhui, China, 2006.
3. K.Y. Li, L.H. Hu, R. Huo, Y.Z. Li, Z.B. Chen, X.Q. Sun, S.C. Li, A Mathematical Model on Interaction of Smoke Layer with Sprinkler Spray, Fire Saf. J. 44 (2009) 96–105. DOI:10.1016/j.firesaf.2008.04.003
4. L.Y. Cooper, The Interaction of an Isolated Sprinkler Spray and a Two-Layer Compartment Fire Environment, Int. J. Heat Mass Tran. 38 (1995) 679–690. DOI:10.1016/0017-9310(94)00188-2
5. L.Y. Cooper, The Interaction of an Isolated Sprinkler Spray and a Two-Layer Compartment Fire Environment. Phenomena and Model Simulations, Fire Saf. J. 25 (1995) 89–107. DOI:10.1016/0379-7112(95)00037-2
6. K.B. McGrattan, A. Hamins, D. Stroup, Sprinkler, Smoke & Heat Vent, Draft Curtain

- Interaction - Large Scale Experiments and Model Development, National Institute of Standards and Technology, Gaithersburg, MD, 1998.
7. W.K. Chow, A.C. Tang, Experimental Studies on Sprinkler Water Spray-Smoke Layer Interaction, J. Appl. Fire Sci. 4 (1995) 171-184.
 8. NFPA13, Standard for the Installation of Sprinkler System, 2002 Ed., National Fire Protection Association, USA, 2002.
 9. L. Yi, Study on Smoke Movement and Management in Atrium Building, PhD dissertation, University of Science and Technology of China, Hefei, Anhui, China, 2005

NOMENCLATURE

| | |
|------------|--|
| B_0 | buoyancy on the smoke layer column element below the sprinkler, N |
| B_L | buoyancy of unit volume at the smoke-air interface, N |
| B_t | total buoyancy of the interaction region when smoke layer is stable, N |
| B_{x1} | buoyancy on the smoke layer column element with unit area, N |
| C_D | drag coefficient |
| d_d | diameter of the droplet, m |
| d_m | mean diameter of all droplets, m |
| D_0 | drag force on the smoke layer column element below the sprinkler, N |
| D_L | drag force of unit volume at the smoke-air interface, N |
| D_t | total drag force of the interaction region when smoke layer is stable, N |
| D_{x1} | drag force on the smoke layer column element with unit area, N |
| E | coefficient of curve equation for the external shape of the spray region |
| g | acceleration due to gravity, ms^{-2} |
| h | initial thickness of the smoke layer, m |
| k_d | coefficient for calculating the drag force of droplet, ms^{-1} |
| m_d | mass of the droplet, kg |
| \dot{M} | discharge mass flow rate of the sprinkler nozzle, kgs^{-1} |
| p_d | operating pressure of the sprinkler, MPa |
| ΔT | average temperature rise of the smoke layer, K |
| T_0 | ambient temperature, K |
| T_L | smoke temperature at the smoke-air interface, K |
| x_1 | coordinate x of the apex of the smoke layer column element, m |

Greek symbols

| | |
|----------|--|
| ρ_d | density of the water, kgm^{-3} |
| ρ_g | density of the smoke, kgm^{-3} |
| ρ_0 | density of the air at ambient temperature, kgm^{-3} |